DESIGN AND TEST EVALUATION OF THE SUBSOILER EQUIPPED WITH TILLAGE DEPTH MONITORING AND CONTROL SUBSOILING ASSEMBLIES
/
耕深自动监测控制深松机深松单体设计与试验

Lou Shangyi[1)], He Jin*[1)], Li Hongwen[1)], Wang Qingjie[1)], Lu Caiyun[1)], Wu Yihang[1)], Liu Peng[1)], Li Hui[2)]
[1)] College of Engineering, China Agricultural University, Beijing 100080 / China;
[2)] Shandong Academy of Agricultural Machinery Sciences, Jinan, 250100 / China
Tel: +8610 62737300; E-mail: hejin@cau.edu.cn
DOI: https://doi.org/10.35633/inmateh-65-15

Keywords: *subsoiler, hydraulic adjustment, stability of tillage depth, subsoiling quality, performance*

ABSTRACT
Aiming at solving problems that the variation of tillage depth between rows and within rows caused by the surface undulation was great, the lateral stability of tillage depth obtained by the method of adjusting at the three-point suspension was poor, and lack of subsoilers with the function of accurate detection and adjustment of single row tillage depth, a method of independent control of single row tillage depth based on ultrasonic sensor detection and hydraulic adjustment was proposed. And the tillage depth monitoring and control subsoiling assembly and the subsoiler equipped with subsoiling assemblies were designed. The key structural parameters of the hydraulic cylinder and the model of the three-position four-way magnetic exchange valve were determined. The subsoiling quality and performance comparison tests were conducted, and the results showed that the mean value of the variable coefficient of soil hardness, looseness of soil and coefficient of soil disturbance were 52.23%, 32.55% and 62.15%, respectively, and the stability coefficient of tillage depth was 92.43%, which all met the subsoiling operation requirements. The standard deviation of tillage depth belonged to the method of independent adjustment of single row and unified adjustment of each row were 38.315mm and 51.521mm, respectively. The subsoiler equipped with tillage depth monitoring and control subsoiling assemblies designed in this paper was capable of significantly improving the stability of tillage depth between rows and within rows.

ABSTRACT
为了解决由于地表起伏造成的深松机行间、行内耕深变异较大，且整机调节方式得到的耕深横向稳定性较差，缺乏实现单行耕深精准检测与调节的深松机的问题，本文提出了一种基于超声波传感器检测与液压调节的独立控制单行耕深的方法，设计了耕深监测控制深松单体以及由多个单体组成的深松机，确定了液压缸的关键结构参数以及三位四通电磁换向阀的型号，开展了深松效果与性能对比试验，结果表明深松前后土壤硬度变化系数均值为 52.23%，土壤蓬松度均值为 32.55%，土壤扰动系数均值为 62.15%，耕深稳定性系数为 92.43%，各项指标均满足深松作业要求，单体调节与整机调节的耕深标准差分别为 38.315mm 和 51.521mm，本文设计的具有单行耕深独立检测与调节功能的深松机能够显著提高行间、行内耕深稳定性。

INTRODUCTION

Cultivated land is the important basis and guarantee of crop production, as well as the foundation to ensure food security (*Poehlitz et al., 2019)*. However, due to continuous ploughing and compaction, the soil compacted hardpan is formed, which prevents the roots from extending to the deeper soil, reduces the absorption of water and fertilizer by roots, hinders the flow of moisture and air, and thus decreases the crop yield (*Somerville et al., 2018; Hargreaves et al., 2019; Kristoffersen et al., 2005)*. Conservation tillage is capable of significantly improving soil properties, reducing wind and water erosion as well as surface runoff, and thus protecting the soil effectively (*He et al., 2018)*. The subsoiling technology is one of the key techniques of conservation tillage, which applies subsoiling machines to loosen the soil without turning over the soil *(Singh et al., 2019)*. Especially the loosening quality on the deeper layer is remarkable. Compared to the plough and rotary tillage, the subsoiling has several advantages, including breaking the soil compacted hardpan, reducing soil bulk density, improving soil porosity, enhancing water storage capacity, increasing soil fertility and water use efficiency, and thus improving crop yields (*Feng et al., 2018; Zhang et al., 2015)*.

The subsoiling depth is a significant index affecting the subsoiling quality and energy efficiency, while it is also an important consideration basis for the government to carry out subsoiling subsidies in China. In the process of operation, subsoiling with insufficient depth cannot break the compacted hardpan completely, and thus the soil properties still need to be improved. Meanwhile, subsoiling with excessive depth increases power consumption and operation cost, resulting in the reduction of energy efficiency. Therefore, it is of prime importance to develop a subsoiler with the function of on-line detection and control of tillage depth.

At present, sensors used to detect tillage depth mainly include tilt sensors and ultrasonic sensors (*Suomi et al., 2015; Yin et al., 2018; Mouazen et al., 2004; Gao et al., 2013*), and the adjustment of tillage depth is mainly realized by applying the hydraulic mechanism or motor mechanism (*Lee et al., 1998; Zhao et al., 2015; Ayiding et al., 2013*). The method, applying tilt sensor to measure the angle change of profiling mechanism and calculating the mathematical model to get the tillage depth, results in the mismatch between the adjustment completion point of tillage depth and the detection point, which caused by the profiling mechanism is generally placed behind the tillage component. While the ultrasonic sensor is commonly installed in front of the tillage component to complete the measurement of the distance between the soil surface and the frame, which avoids the inaccuracy caused by the profiling lagging. This method aims at adjusting the tillage depth of the whole machine or a group of tillage components of the combined scarification equipment, which is the same as the objective of mounting the tilt sensor on the three-point suspension to detect angle change of the lifting arm or drawbar. However, due to surface relief or soil resistance variation, there exists the problem of lateral instability of tillage depth of the machine with several shanks, which leads to the inconsistency of soil conditions in the lateral distribution. Therefore, it is necessary to develop a special assembly structure of subsoiling components that is capable of independently adjusting tillage depth of each row.

Hence, in order to avoid undesirable tillage depth of each shank and improve consistency of tillage depth between shanks during the subsoiler operation, in this paper, we proposed a method for independent adjustment of single row tillage depth based on ultrasonic sensor detection and hydraulic adjustment. And the single subsoiling assembly capable of monitoring and controlling tillage depth and the subsoiler equipped with subsoiling assemblies were designed. Furthermore, the subsoiling performance of the tillage depth monitoring and control subsoiler was evaluated by testing the qualified indexes, and the improvement effect of this subsoiler on the stability of single row tillage depth was verified by conducting the performance comparison test.

MATERIALS AND METHODS

Structure and working principle

The overall structure of the subsoiler is shown in Fig.1a); it consists of a frame and four tillage depth monitoring and control subsoiling assemblies. The tillage depth of each shank is independently detected, displayed, recorded and adjusted.

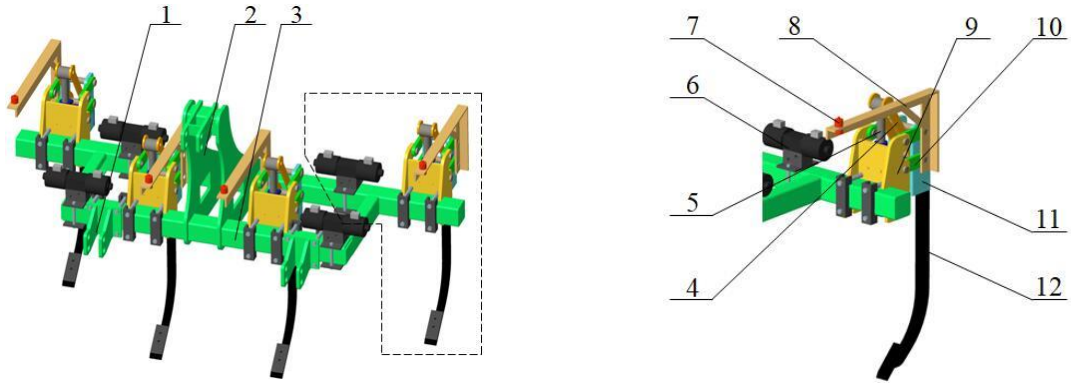

a) Overall structure of the subsoiler **b) Structure of the single subsoiling assembly**

Fig. 1- Structure of the subsoiler equipped with tillage depth monitoring and control subsoiling assemblies

1. Lower suspension point; 2. Upper suspension point; 3. Frame; 4. Hydraulic linkage; 5. Hydraulic cylinder; 6. Magnetic exchange valve; 7. Ultrasonic sensor; 8. Sensor bracket; 9. Fixed mount; 10. Swing rod; 11. Connect plate of the shank; 12. Subsoiler shank

The length, width and height of the subsoiler are 2200mm, 1130mm and 1492mm, respectively. The spacing of two lower suspension points is 982mm, the vertical spacing between the upper and lower suspension point is 624mm, and the range of operation row-spacing is 550~650mm.

The structure of the single subsoiling assembly is shown in Fig.1b); it is composed of a fixed mount, a hydraulic cylinder, two hydraulic linkages, four swing rods, a connect plate of the shank, a subsoiler shank, an ultrasonic sensor, a sensor bracket, and a magnetic exchange valve. The fixed mount was installed on the frame, other parts of the subsoiling assembly were fixed on or connected with the fixed mount, and the main body of the subsoiling assembly was integrated with the frame. The hydraulic cylinder was vertically fixed on the plant between the plates on both sides of the fixed mount. Swing rods were used to connect the fixed mount and the connect plate of the shank, and hydraulic linkages were used to connect the hydraulic cylinder and the connect plate of the shank. The subsoiler shank was fixed on the connect plate of the shank. This combined structure enables the shank to lift or lower in the vertical direction when the hydraulic cylinder is extended or shortened, and thus the tillage depth is reduced or increased to reach desirable value. The sensor bracket was mounted on the side of the connect plate of the shank, and the ultrasonic sensor applied to measure its distance from the soil surface was installed at the front of it, which ensures the synchronous up and down movement of the sensor and the shank. The magnetic exchange valve was fixed on the frame.

In addition to the ultrasonic sensor and magnetic exchange valve, the hardware of the control system of the subsoiler also included an analogue input module, a controller and an interactive touch screen. The analogue input module (S7-200SMART EM AI04, China) was applied in this study, which was used to convert the analogue signal outputted from the ultrasonic sensor into digital signal. The programmable logic controller (S7-200SMART, CPU ST40, China) and interactive touch screen (MT6071iP, China) were applied in this study. The PLC outputted control signal to the drive circuit of the magnetic exchange valve to adjust the tillage depth within the set range, which was inputted via the interactive touch screen. The real-time tillage depth was displayed via the interactive touch screen and recorded on a USB flash disk. The block diagram of monitoring and control system was shown in Fig.2.

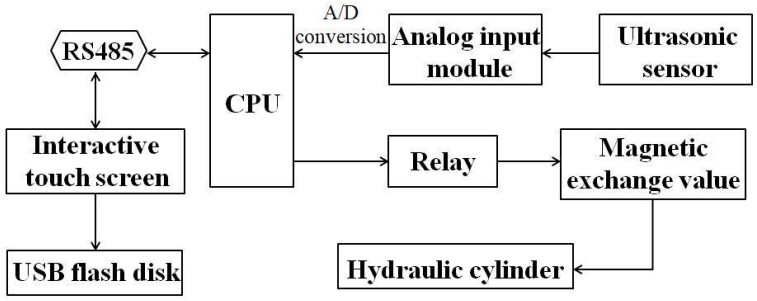

Fig. 2- Block diagram of monitoring and control system

The circuit elements, analogue input module, PLC and interactive touch screen, were placed in the tractor cab, which were powered by the on-board battery. The hydraulic cylinders of the tillage depth monitoring and control subsoiling assemblies were supplied by the tractor's hydraulic system, the hydraulic oil of which was transported through multiple hydraulic output ports. The driving circuit of the three-position four-way magnetic exchange valve controlled the valve position of the magnetic exchange valve to determine the flow direction of hydraulic oil. The desirable tillage depth was set via the interactive touch screen according to the local required depth value. During the subsoiling operation, ultrasonic sensors respectively detected their distance from the surface and sent corresponding signal to the control system. The magnetic exchange valves responded to the output signal of the control system, opening left or right valves or holding in middle position, to make the hydraulic cylinder complete the telescopic movement or remain unchanged. And thus, the tillage depth of each subsoiler shank was independently detected and adjusted to match the set range.

Design of key component parameters

Design of the subsoiler shank

The chisel subsoiler is adaptive for equipping with tillage depth monitoring and control system, so the subsoiler designed in this study initially adopted the common chisel shank, of which the optimization design had been conducted to achieve the purpose of reducing tillage resistance in the process of upper and lower adjustment. The chisel shank is composed of the handle and tip, and there are three kinds of handle that are commonly used, vertical column type, curved type and arc type. The first two type shanks are not suitable to be used in conservation field with more straw and stubble, while the arc type handle with front edge is capable of cutting on the stubble, so the object of optimization design of shank in this study is the chisel shank with arc type handle. Aiming at decreasing resistance of the shank during the subsoiling operation as well as lifting or

lowering adjustment, the force analysis of the shank in the process of operation was carried out, and the equivalent stress were analysed by the finite element method. Based on these, the sources increasing the tillage resistance caused by the structural parameters of the shank tip and shank handle were found out, and the optimization design of shank was conducted to reduce the tillage resistance. The resistance of the shank (F) was given by Eq.(1). The resistance of the shank tip was derived by the Eqs.(2)-(4), and the resistance of the shank handle was calculated by the Eq.(5) (*Yu et al., 2007*).

$$F = F_1 + F_2 \tag{1}$$

where:

F_1 is the resistance of the shank tip, [N];

F_2 is the resistance of the shank handle, [N].

$$F_1 = \frac{G}{t_2} + \frac{t_1}{t_2\left(\sin\beta + \mu_1\cos\beta\right)} \tag{2}$$

$$t_1 = \frac{Cbd\left(1+\tan\frac{\delta}{8}\right)}{\sin\beta} \tag{3}$$

$$t_2 = \frac{\cos\delta - \sin\delta}{\sin\delta + \cos\delta} + \frac{\cos\beta - \sin\beta}{\sin\beta + \cos\beta} \tag{4}$$

$$F_2 = 2N_2\sin\frac{\alpha}{2} + 2N_2\mu_2\cos\frac{\alpha}{2} + 2N_3\mu_2 \tag{5}$$

where:

F_1 is the resistance of the shank tip, [N];

F_2 - resistance of the shank handle, [N];

G - gravity of soil on the shank, [N];

α - cutting edge inclination, [°];

β - inclination of the front failure surface, [°];

δ - penetration angle of the shank, [°];

d - tillage depth, [cm];

b - shank width, [cm];

μ_1 - friction coefficient between the surface of the shank tip and soil;

μ_2 - friction coefficient between soils;

C - unit cohesion of soil, [N·cm^{-2}];

N_2 - normal load on the front bevel of the shank handle, [N];

N_3 - normal load on the side of the shank handle, [N].

The soil bulk density was selected to be 1.45×10^3 kg·m^{-3}, the angle between the lower surface of the shank tip and the horizontal direction was 10°, the penetration angle of the shank was 23°, the width and length of the shank tip was 50mm and 165mm, respectively, the friction coefficient between the surface of the shank tip and soil was selected to be 0.6, the friction coefficient between soils was selected to be 0.3, and the unit cohesion of soil was selected to be 2 N·cm^{-2}.

Aiming at obtaining tillage depth within the set range during the subsoiling operation, undesirable depth should be adjusted to meet the requirement. Setting that the desirable tillage depth was from 250 mm to 450 mm, and the initial tillage depth was selected as 350 mm. When the field surface was flat, the tillage depth remained roughly the same, and the system controlled the shank position unchanged. The F_1 calculated by the Eqs.(2)-(4) was 816 N when the tillage depth was 350mm, the F_2 calculated by the Eq.(5) was 3004 N, and the F calculated by the Eq.(1) was 3820 N. When the field surface was uneven, the tillage depth suddenly increased to about 500 mm, which was greater than the set maximum value, the shank needed to be raised, and until the tillage depth was about 250 mm, the maximum amount of lifting was achieved. When the tillage depth was about 500 mm, the calculated F_1 was 927 N, the calculated F_2 was 4021 N, and thus the calculated force F was 4948 N. When the tillage depth was about 250 mm, the calculated F_1 was 534 N, the calculated F_2 was 2680 N, and thus the calculated F was 3214 N. While when the tillage depth suddenly reduced from

350 mm to about 200 mm, which was less than the set minimum value, the shank needed to be lowered. Until the tillage depth was about 350 mm, the calculated F_1 was 850N, the calculated F_2 was 3147 N, and thus the calculated F was 3997 N.

The three-dimensional model of shank was imported into the finite element analysis software to solve the equivalent stress. The method of Fixed Support was used to add fixed constraint on the installation position of the shank, and the force was applied on the shank tip and handle according to the above calculated values. The results of solution showed that the maximum stress and deformation of the shank was 244.83MPa and 4.213mm, respectively. With the increase of tillage depth, the maximum stress of the shank increased with the raise of tillage resistance. Therefore, it is necessary to optimize the structure of the shank to reduce the tillage resistance during subsoiling operation, and slow down the stress increase of the shank in the process of lowering adjustment. According to Eqs.(2)-(5), the decrease of F_1 and F_2 is enabled by respectively reducing the value of G and N_2. The width of the shank was optimized from 50mm to 40mm, as well as the length was optimized from 165mm to 155mm, to reduce the area of soil acting on the shank tip, which was capable of reducing the value of G. The bottom side of the shank handle was designed as a rhombus to decrease the value of N_2, and thus reducing the force of the soil on the bottom of the shank handle. The finite element analysis was also carried out to solve the equivalent stress of the optimized shank, and the results showed that the maximum equivalent stress of the shank was 214.38 MPa, which is less than the 244.83 MPa. The equivalent stress and deformation distribution diagram of the unaltered shank and optimized shank were shown in Fig.3 and Fig.4, respectively.

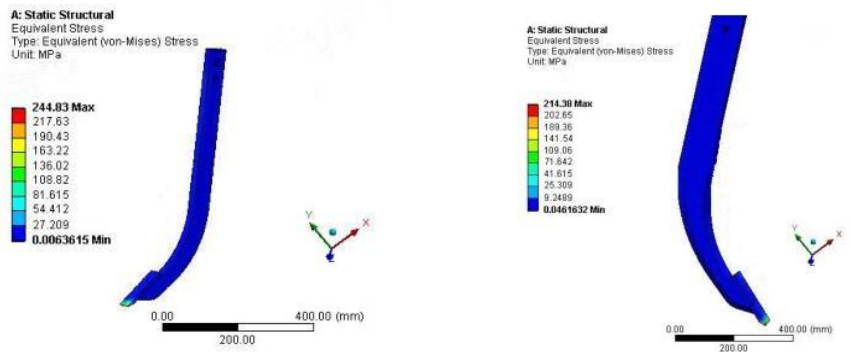

(a) **(b)**

Fig. 3 - Comparison of equivalent stress distribution between the unaltered shank (a) and optimized shank (b)

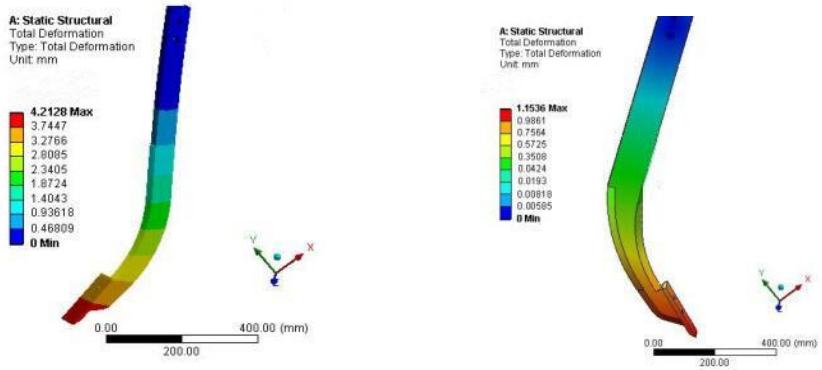

(a) **(b)**

Fig. 4 - Comparison of deformation distribution between the unaltered shank (a) and optimized shank (b)

Design of the fixed mount and connect plate of the shank

The fixed mount and connect plate of the shank are the major components to fix the subsoiling assembly on the frame and enable good match between parts. The stability and reliability of these two components is the key to ensure efficient operation of the subsoiler. Two parallel four-bar mechanisms was respectively composed of a fixed mount, two swing rods and a connect plate of shank, which was capable of converting the telescopic movement of the hydraulic cylinder into the vertical up and down movement of the subsoiler shank.

According to the above structural and functional requirements, the basic structure of the fixed mount was designed, and its schematic diagram and force was shown in Fig.5. F_1 and F_2 were the support reaction of the swing rods, M_1 and M_2 were the flexural moment at the position of the hinge pins, P was the support reaction of the hydraulic mechanism, M_p was the flexural moment at the mounting hole of the U-bolt used to fix the hydraulic cylinder, F was the supporting force of the frame to the subsoiling assembly, and M was the flexural moment of the subsoiling assembly fixed on the frame. The fixed mount is made of No.45 steel, the elastic modulus of which is 2.09×10^{11} N/m and the yield strength is 355 MPa. The total weight of the subsoiling assembly was about 55 kg, and the support reaction of the swing rods was about 5460 N. The diameter of each hole and the distance between the hole and the boundary of the fixed mount were determined by Eqs.(6)-(7).

$$\tau=\frac{F}{A}\leq[\tau] \tag{6}$$

where:

τ is the shear stress, [MPa];

F - the shear force, [kN];

A - the shear area, [mm^2].

$$\sigma_{r3}=\frac{\sqrt{M^2+T^2}}{W}\leq[\sigma] \tag{7}$$

where:

M is the flexural moment, [kN·m];

T is the torque, [N·m];

W is the section modulus in bending, [mm^3].

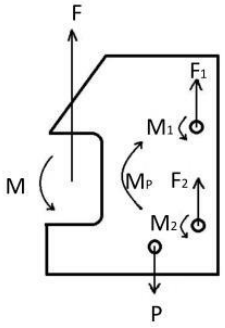

Fig. 5 - Schematic diagram of structure and force

The diameter of the hole for passing through the hinge pin used to install the swing rod was 20mm, and the distance of the hole from the boundary of the fixed mount must be greater than or equal to 16mm. Meanwhile, the diameter of the hole for passing through the hinge pin used to fix the hydraulic cylinder was 25mm and the diameter of the hole for inserting the u-bolt was13mm, while the distance of the hole from the boundary of the fixed mount can't be less than 20mm. Furthermore, the overall dimension of the fixed mount was determined, including length, width and height.

Taking structural parameters and operating parameters into consideration, the distance between the front beam and the back beam of the frame was 400mm, the operation spacing ranged from 500mm to 700mm, and the maximum vertical displacement of the shank in the adjustment process was 200mm, the length, width and height of the fixed mount should not be larger than 250mm, 200mm and 360mm, respectively. In order to improve stiffness of the fixed mount, topology optimization was carried out using OptiStruct software, and the initial model in topology optimization was shown in Fig.6. The flexibility of the fixed mount was taken as the target response, the optimization region was taken as the design variable, and the volume ratio was set as the constraint. The volume ratio of 80%, 85% and 90% were selected as the upper limit for trial operation, and up to 85% of the volume belonging to the three-dimensional model was retained, which depends on the overall maximum stress that was considered as comparison parameter.

The positions of hinge holes and pin holes were changed, and the topology optimized model, the stress of which was reduced and the stiffness improved, was shown in Fig.7.

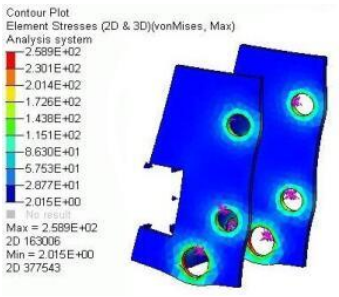

Fig. 6- Initial model

Fig. 7- Topology optimized model

The connect plate of the shank was stressed at the hinge holes and bolt holes, which were respectively used to connect the swing rods and fix the shank. It is made of No.45 steel, its material properties are the same as those of the fixed mount. The thickness of the steel plate used for the connect plate of the shank was 10 mm, and the diameter of the hinge hole was 25mm as well as of the bolt hole was 15mm. Static analysis results of the connect plate of the shank showed that its maximum stress was much less than the allowable stress, and the maximum deformation was 0.137mm. The material and structure of the connect plate of the shank met the request for utilization.

Design of the hydraulic linkage and swing rod

Each subsoiling assembly had four swing rods and two hydraulic linkages. One side of the swing rod was hinged with the fixed mount, and another side was hinged with the connect plate of shank. While one side of the hydraulic linkage was hinged with the hydraulic cylinder shaft, the other side was hinged with the lower swing rod. In this study, the stroke of the hydraulic cylinder was required to be 200mm, and the displacement of the upper and lower adjustment was 100mm, respectively. The relationship between the stroke of the hydraulic cylinder, the length of the swing rod and hydraulic linkage was presented in Eq.(8).

$$L=r\left(1-\cos\theta\right)+\frac{r^2}{l}\left(1-\cos 2\theta\right) \tag{8}$$

where:

L is the stroke of the hydraulic cylinder, [mm];

r the length of the swing rod, [mm];

l - the length of the hydraulic linkage, [mm];

θ - the rotation angle of the swing rod, [°].

The required stroke of the hydraulic cylinder was 200mm, the rotation angle of the swing rod ranged from 45° to 125°, and the range of the rotation angle of the hydraulic linkage was 26°~35°. After calculation, the length of the swing rod and hydraulic linkage was 140mm and 383mm, respectively. The swing rod and hydraulic linkage were made of No.45 steel, and the thickness of the swing rod and hydraulic linkage was determined to be 10mm.

Determination of the hydraulic cylinder and magnetic exchange valve

The effective working area of the piston was derived by the Eqs.(9)-(10) (*Cheng et al., 2008*).

$$F = F_L + F_f + F_a \tag{9}$$

where:

F is the total load applied on the hydraulic cylinder, [N];

F_L - workload applied on the hydraulic cylinder, [N];

F_f - frictional resistance applied on the hydraulic cylinder, [N];

F_a - inertia load applied on the hydraulic cylinder, [N].

$$A = \frac{F}{P} \tag{10}$$

where:

A is the effective working area of the piston, [mm^2];

F is the total load applied on the hydraulic cylinder, [N];

P is the working pressure of the hydraulic cylinder, [MPa].

$$D = \sqrt{\frac{4A}{\pi}} \tag{11}$$

where D is the diameter length of the effective working area.

The subsoiler designed in this study had four rows of shanks, and each shank was separately equipped with a group of hydraulic transmission mechanism, the working pressure of which was determined to be 12MPa. The effective working area of the piston was calculated to be 583.33 mm^2, so the D was equal to 27.25mm.

According to the standard table, the inner diameter of the hydraulic cylinder was selected to be 32mm. Besides, the rod diameter of the hydraulic cylinder was 20mm, the outer diameter of the hydraulic cylinder was 55mm, and the stroke of the hydraulic cylinder was 200mm.

The type of the magnetic exchange valve was determined according to the working parameters and motion state of the hydraulic cylinder. In order to reduce the tillage depth when it's larger than the desirable value, increase the depth when it's less than the desirable value, and keep the depth unchanged when it's at the desirable value, the hydraulic cylinder needs to complete three actions, elongation, shortening and remaining unchanged. So, the three-position four-way magnetic exchange valve (DSG-03-3C60-DL-DC24) was applied in this study, which was controlled to open the left and right valves or keep the middle position to complete the telescopic movement of the hydraulic cylinder, and thus the desirable tillage depth was obtained by lifting or lowering the shank or keeping the position of the shank unchanged. The rated flow of this type of magnetic exchange valve is 60L/min, the maximum flow is 100 L/min, and the maximum working pressure is 24.5MPa.

Design of the sensor bracket

During the subsoiling operation, the speed of the tractor was about 3~5km/h, while the monitoring and control period of the system was 1s and the response time of the system was 0.4s. Within the response time, the advance distance of the subsoiler was given by Eq.(12).

$$S = v \times t \tag{12}$$

where:

S is the advance distance of the subsoiler, [m];

v - the speed of the tractor, [m/s];

T - the response time, [s].

Therefore, the range of advance distance in response time was 0.33~0.56m. In order to avoid profile lag, the ultrasonic sensor on the sensor bracket should be installed in front of the shank tip in the forward direction, and the distance between them basically enabled the same as the displacement of the subsoiler from current position to the detection point within the response time. The sensor bracket was fixed on the one side of the connect plate of the shank, which was capable of moving up and down synchronously with the shank, and the ultrasonic sensor was installed at the end of the forward extension part of it, as shown in Fig.8. To avoid the negative impact of vibration on the detection accuracy of tillage depth during the subsoiling operation, the forward extension distance of the sensor bracket was set as 500mm.

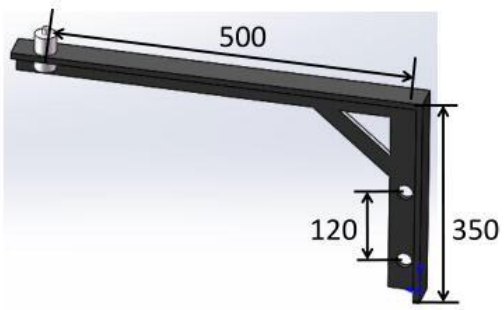

Fig. 8- Structure of the sensor bracket with the ultrasonic sensor

Evaluation experiment

Test arrangement

The field experiments were conducted to evaluate the subsoiling quality and operation performance of the subsoiler equipped with tillage depth monitoring and control subsoiling assemblies, and test indexes included the variable coefficient of soil hardness, looseness of soil, coefficient of soil disturbance and stability coefficient of tillage depth. Meanwhile, the comparison test of two adjustment methods was carried out, including independent adjustment of single row and unified adjustment of each row. The field experiments were carried out in Shenze County, Hebei Province, North China. Maize straw was returned to the field, and the soil type belongs to fluro-aquil soil. The mean value of the soil moisture and soil bulk density was 15.4% and 1.45 g/cm³, respectively. The subsoiler equipped with tillage depth monitoring and control subsoiling assemblies was driven by the Levo TG series M1254-G tractor. The field experiment was shown in Fig.9.

Fig. 9 - Field experiments

1. Fixed mount; 2. Hydraulic cylinder; 3. Frame; 4. Magnetic exchange valve; 5. Sensor bracket; 6. Tractor; 7. Hydraulic linkage; 8. Ultrasonic sensor; 9. Swing rod; 10. Connect plate of the shank; 11. Subsoiler shank

Subsoiling quality test

Soil hardness is one of the important physical properties of soil. Comparing between subsoiled soil and unsubsoiled soil, the larger the variable coefficient of soil hardness is, the greater the change of soil hardness will be, and thus better subsoiling quality is obtained. The variable coefficient of soil hardness was given by Eq.(13). Looseness of soil, coefficient of soil disturbance and stability coefficient of tillage depth are significant indexes to evaluate subsoiling quality. Looseness of soil and coefficient of soil disturbance was respectively obtained by Eq.(14) and Eq.(15), and stability coefficient of tillage depth was derived by Eqs.(16) - (19).

$$C = \frac{H - H_i}{H} \times 100\% \tag{13}$$

where: C represents the variable coefficient of soil hardness, [%];

H represents the soil hardness before subsoiling, [kg/cm^2];

H_i represents the soil hardness after subsoiling, [kg/cm^2].

$$P = \frac{A_h - A_q}{A_q} \times 100\% \tag{14}$$

$$Y = \frac{A_s}{A_q} \times 100\% \tag{15}$$

where: P represents the looseness of soil, [%];

Y represents the coefficient of soil disturbance, [%];

A_h represents the section area between the theoretical curve of the furrow bottom and the surface curve of the subsoiled soil, [cm^2];

A_q represents the section area between the theoretical curve of the furrow bottom and the surface curve of the unsubsoiled soil, [cm^2];

A_s represents the section area between the actual curve of the furrow bottom and the surface curve of the subsoiled soil, [cm^2].

$$a = \frac{\sum a_i}{n} \tag{16}$$

$$S = \frac{\sqrt{\sum (a_i - a)^2}}{n-1} \tag{17}$$

$$V = \frac{S}{a} \times 100\% \tag{18}$$

$$U = 1 - V \tag{19}$$

where:

a represents the average value of the tillage depth, [mm];

a_i represents the tillage depth of each measuring point, [mm];

n represents the number of the selected points measured manually;

S represents the standard deviation of tillage depth, [mm];

V represents the variation coefficient of tillage depth stability, [%];

U represents the stability coefficient of tillage depth, [%].

Three points were randomly selected from a row within the 50m length of the subsequent subsoiling operation section, and the soil hardness of each point at three soil layers was measured by the soil hardness instrument, including depth of 0~15cm, 15~30cm and 30~45cm. The position of each point was marked, the soil hardness data were recorded and the average soil hardness of each depth layer was calculated.

The subsoiler equipped with tillage depth monitoring and control subsoiling assemblies advanced 50m at the speed of 5 km/h, and the tillage depth range was set at 350~450 mm. After subsoiling, the soil hardness of three depth layers at three marked positions were measured and recorded, and the average soil hardness of each depth layer was obtained.

Therefore, the variable coefficient of soil hardness was solved by substituting the relevant data into Eq.(13). A part of the subsoiling area was selected to dig out the soil and show the furrow cross-section, and the surface curve of the unsubsoiled soil, the surface curve of the subsoiled soil and the curve of the furrow bottom were drawn with the same horizontal line in the furrow cross-section. A_h, A_q and A_s was calculated, and thus looseness of soil and coefficient of soil disturbance was respectively obtained by substituting the relevant value into Eq.(14) and Eq.(15).

Along the subsoiling operation route, 30 points were selected every 1.4m from the starting position and their tillage depth was measured manually. Substituting the relevant data into Eqs.(16)-(19), stability coefficient of tillage depth was calculated.

Performance comparison test

Performance comparison test was carried out on the subsoiler equipped with subsoiling assemblies under two adjustment modes of tillage depth, including automatic detection and adjustment of single row tillage depth controlled by the system and adjustment at three-point suspension by the tractor, to verify the improvement effect of the subsoiler equipped with tillage depth monitoring and control subsoiling assemblies on the stability of single row tillage depth. The tillage depth range was set at 250~450 mm. The subsoiler advanced 50 m at a speed of 5 km/h under the system operation state and the system stopped operation state, respectively. After the subsoiling operation, 10 measuring points were selected at equal distance from each operation route for manual measurement of tillage depth, and then these data were analysed and compared.

RESULTS AND DISCUSSION

Results of subsoiling quality test

Mean value of soil hardness of each soil layer at three marked points, and the variable coefficient of soil hardness of each soil layer before and after subsoiling were shown in Table1, while looseness of soil and coefficient of soil disturbance were given in Table 2.

Table 1

Soil hardness and variable coefficient of soil hardness before and after subsoiling

Soil depth [cm]	Soil hardness before subsoiling [kg/cm^2]	Soil hardness after subsoiling [kg/cm^2]	Variable coefficient of soil hardness [%]
0~15	15.88	5.78	63.60
15~30	20.13	10.21	49.28
30~45	27.85	15.65	43.81
Mean value	21.29	10.55	52.23

Table 2

Looseness of soil and coefficient of soil disturbance

Set depth range [mm]	A_h [cm^2]	A_q [cm^2]	A_s [cm^2]	Looseness of soil [%]	Coefficient of soil disturbance [%]
350~450	42.74	32.31	20.06	32.55	62.15

According to the data in the Table 1, the mean value of the variable coefficient of soil hardness among the three depth layers was 52.23%, which illustrated that the soil hardness was significantly reduced after subsoiling operation of the subsoiler equipped with tillage depth monitoring and control subsoiling assemblies, which met the requirements of subsoiling operation. Meanwhile, the data in Table 2 showed that looseness of soil was 38.17% and coefficient of soil disturbance was 63.84%, and it indicated that the subsoiler designed in this paper was capable of obtaining good subsoiling quality and the soil which had been subsoiled met the standard requirement. Manually measured tillage depth at 30 selected points along the subsoiling operation route was shown in Fig.11, and the stability coefficient of tillage depth was 92.43% based on the derivation of Eqs.(16) - (19), which was more than 85% and met the requirement of depth stability in subsoiling operation.

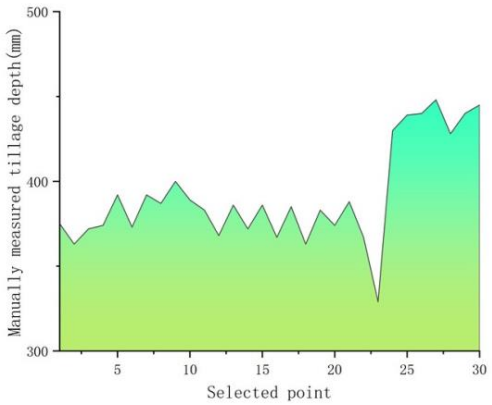

Fig. 10 - Manually measured tillage depth at 30 selected points

It was obvious in Fig.10 that the tillage depth between the first point and the 22nd point and between the 24th point and the 30th point basically remained unchanged. However, the tillage depth of the 23rd point was much smaller than that of the 22nd point. This might be due to the fact that there was depression on the surface, which made the tillage depth decrease greatly and led to the large difference of the tillage depth. Fortunately, the tillage depth monitoring and control system played a significant role in adjusting the tillage depth from 329mm to 430mm in time, which made the tillage depth meet the set range and improve the stability of tillage depth.

Results of performance comparison test

The tillage depth of 10 points selected equidistantly along each subsoiling route, which was respectively generated under the system operation state and the system stopped operation state, were shown in Fig.11. The standard deviation of tillage depth obtained by the method of adjusting the single shank was 38.315mm, while the standard deviation of tillage depth obtained by the method of adjusting the whole machine was 51.521mm, which indicated that the discreteness of the data obtained by the second method was greater than that by the first method. It was shown in Fig.11 that the minimum tillage depth was 221.5mm and the maximum tillage depth was 332.8mm, which were obtained by adjusting the single shank.

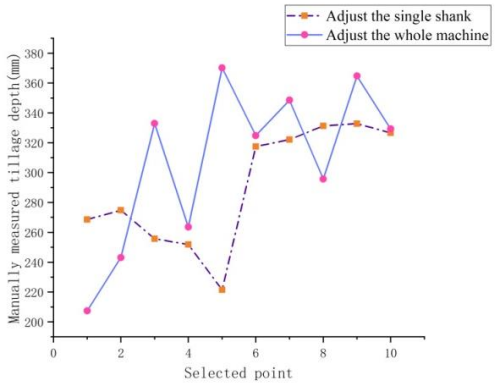

Fig. 11 - Comparison of tillage depth under two adjustment methods

The tillage depth of the first point to the fourth point was almost equal, and so was the tillage depth from the sixth point to the tenth point. These data were all within the set range of tillage depth. Nevertheless, due to the sunken surface between the fourth and fifth point, the tillage depth was reduced to 221.5mm and it was less than the minimum value of the set range, which was 250mm. The system controlled the hydraulic cylinder shortening to lower the shank so that the tillage depth was adjusted from 221.5mm to 317.5mm in time to make the tillage depth within the set range. Meanwhile, the minimum tillage depth was 207.4mm and the maximum tillage depth was 370.2mm, which were obtained by adjusting at the three-point suspension depending on the tractor driver, and tillage depth of four points were all outside the set range. The tillage depth at the first point was 207.4mm and at the second point was 243.1mm. It was obvious that when the tillage depth was outside the set range, this adjustment method was incapable of accurately adjusting the tillage depth to the desirable value. Besides, cross-section of partial subsoiling furrows belonging to these two adjustment methods were shown in Fig.12, which illustrated that compared with the method of adjusting the single shank, the variation of tillage depth obtained by the method of adjusting at the three-point suspension was larger. Hence, the stability of tillage depth obtained by this method was poor and the depth difference was great. It was proved that the subsoiler equipped with tillage depth monitoring and control subsoiling assemblies was capable of improving the tillage depth stability of single row.

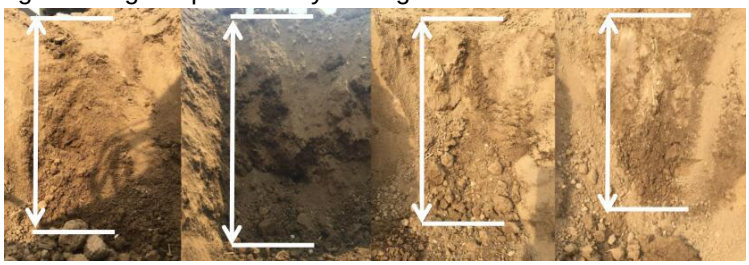

(a)

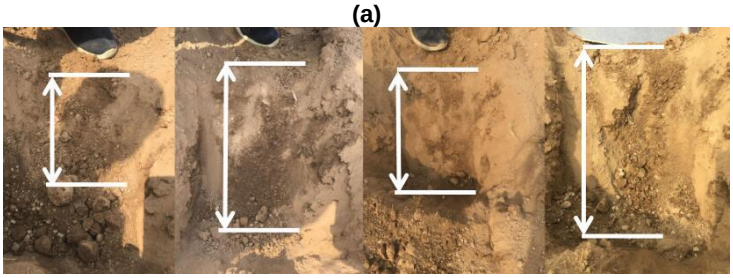

(b)

Fig. 12 - Cross-section of partial subsoiling furrows belongs to the method of adjusting the single shank (a) and adjusting at three-point suspension (b)

CONCLUSIONS

(1) A method for independent control of single row tillage depth based on ultrasonic sensor detection and hydraulic adjustment was proposed. The tillage depth monitoring and control subsoiling assembly and the subsoiler equipped with such assemblies were designed.

(2) Key structural parameters of the hydraulic cylinder were determined via the force analysis of subsoiling assembly. The inner diameter, rod diameter, outer diameter and stroke of the hydraulic cylinder were 32mm, 20mm, 55mm and 200mm, respectively. The three-position four-way magnetic exchange valve was applied to meet the requirement of three operation states of the hydraulic cylinder, including elongation, shortening and remaining unchanged.

(3) The subsoiling quality test was conducted and the results showed that the mean value of the variable coefficient of soil hardness, looseness of soil and coefficient of soil disturbance were 52.23%, 32.55% and 62.15%, respectively. The stability coefficient of tillage depth was 92.43%. The subsoiling quality of the tillage depth monitoring and control subsoiling assembly was good and all indexes met requirements.

(4) The performance comparison test was carried out, and the results indicated that the standard deviation of tillage depth belonging to the method of adjusting the single shank and adjusting at the three-point suspension were 38.315mm and 51.521mm, respectively. It was verified that the stability of single row tillage depth was significantly improved by applying the subsoiler equipped with tillage depth monitoring and control subsoiling assemblies.

ACKNOWLEDGEMENT

The author(s) disclosed receipt of the following financial support for the research, authorship, and/or publication of this article: This work was supported by the Modern Agricultural Industry Technology System (Grant No.CARS-03); The 2115 Talent Development Program of China Agricultural University.

REFERENCES

[1] Ayiding, K., Wu, M.T., He, P.X., Liu, X.R., & Sun, B. (2013). The control system of automatic adjustment for ploughing depth (耕深自动调节控制系统). *Journal of Agricultural Mechanization Research*, 3, 160-163. http://dx.doi.org/10.13427/j.cnki.njyi.2013.03.043

[2] Cheng, D.X., Wang, D.F., Ji, K.S., et al., (2008). Hand book of mechanical design (机械设计手册). *Chemical Industry Press*, Beijing/China.

[3] Feng, X.M., Hao, Y.B., Latifmanesh, H., Lal, R., Cao, T.H., Guo, J.R., Deng, A.X., Song, Z.W., & Zhang, W.J. (2018). Effects of subsoiling tillage on soil properties, maize root distribution, and grain yield on Mollisols of Northeastern China. *Agronomy Journal*, 110(4), 1607-1615. https://doi.org/10.2134/agronj2018.01.0027

[4] Gao, L., Yang, F., Wang, R.T., Jiang, L., Wang, D. (2013). Rotary cultivator digging depth design of detection system (旋耕机松土深度检测系统设计). *Journal of Agricultural Mechanization Research*, 5, 159-162. http://dx.doi.org/10.13427/j.cnki.njyi.2013.05.034

[5] Hargreaves, P.R., Baker, K.L., Graceson, A., Bonnett, S., Ball, B.C., & Cloy, J.M. (2019). Soil compaction effects on grassland silage yields and soil structure under different levels of compaction over three years. *European Journal of Agronomy*, 109, 1-9. https://doi.org/10.1016/j.eja.2019.125916

[6] He, J., Li, H.W., Chen, H.T., Lu, C.Y., & Wang, Q.J. (2018). Research progress of conservation tillage technology and machine (保护性耕作技术与机具研究进展). *Transactions of the Chinese Society for Agricultural Machinery*, 49(4), 1-18. http://dx.doi.org/10.6041/j.issn.1000-1298.2018.04.001

[7] Kristoffersen, A.O., & Riley, H. (2005). Effects of soil compaction and moisture regime on the root and shoot growth and phosphorus uptake of barley plants growing on soils with varying phosphorus status. *Nutrient Cycling in Agroecosystems*, 72(2), 135-146. https://doi.org/10.1007/s10705-005-0240-8

[8] Lee, J., Yamazaki, M., Oidab, A., Nakashimac, H., & Shimizub, H. (1998). Electro-hydraulic tillage depth control system for rotary implements mounted on agricultural tractor Design and response experiments of control system. *Journal of Terramechanics*, 35(4), 229-238. https://doi.org/10.1016/S0022-4898(98)00026-3

[9] Mouazen, A.M., Anthonis, J., Saeys, W., & Ramon, H. (2004). An automatic depth control system for online measurement of spatial variation in soil compaction.1. Sensor design for measurement of frame height variation from soil surface. *Biosystems Engineering*, 89(2), 139-150. http://doi.org/10.1016/j.biosystemseng.2004.06.005

[10] Poehlitz, J., Ruecknagel, J., Schlueter, S., Vogel, H.J., & Christen, O. (2019). Computed tomography as an extension of classical methods in the analysis of soil compaction, exemplified on samples from two tillage treatments and at two moisture tensions. *Geoderma*. *346*, 52-62. https://doi.org/10.1016/j.geoderma.2019.03.023

[11] Singh, k., Choudhary, O.P., Singh, H.P., Singh, A., & Mishra, S.K. (2019). Sub-soiling improves productivity and economic returns of cotton-wheat cropping system. *Soil &Tillage Research*, 189, 131-139. https://doi.org/10.1016/j.still.2019.01.013

[12] Somerville, P.D., May, P.B., & Livesley, S.J. (2018). Effects of deep tillage and municipal green waste compost amendments on soil properties and tree growth in compacted urban soils. *Journal of Environmental Management*, 227, 365-374. https://doi.org/10.1016/j.jenvman.2018.09.004

[13] Suomi, P., & Oksanen, T. (2015). Automatic working depth control for seed drill using ISO 11783 remote control messages. *Computers and Electronics in Agriculture*, 116, 30–35. https://doi.org/10.1016/j.compag.2015.05.016

[14] Yin, Y.X., Wang, C., Meng, Z.J., Chen, J.P., Guo, S.X., & Qin, W.C. (2018). Operation Quality Measurement Method for Tilling Depth of Suspended Subsoiler (悬挂式深松机耕整地耕深检测方法研究). *Transactions of the Chinese Society for Agricultural Machinery*, 49(4), 68-74. http://dx.doi.org/10.6041/j.issn.1000-1298.2018.04.008

[15] Yu, Y.C., Liu, W.Y., Zhao, Y.F., & Sun, J.Q. (2007). Force mathematical model and examination analysis of the column subsoiler (立柱式深松铲受力数学模型及试验分析). *Transactions of the Chinese Society of Agricultural Engineering*, 23(6), 109-113. http://dx.doi.org/10.3969/j.issn.1002-6819.2007. 06.005

[16] Zhang, R.F., Yang, H.S., Gao, J.L., Zhang, Y.Q., Wang, Z.G., Fan, X.Y., & Bi, W.B. (2015). Effect of subsoiling on root morphological and physiological characteristics of spring maize (深松对春玉米根系形态特征和生理特性的影响). *Transactions of the Chinese Society of Agricultural Engineering*, 31(5), 78-84. http://dx.doi.org/10.3969/j.issn.1002-6819.2015.05.012

[17] Zhao, J.H., Liu, L.J., Yang, X.J., Liu, Z.J., Tang, J.X. (2015). Design and laboratory test of control system for depth of furrow opening (播种机开沟深度控制系统的设计与室内试验). *Transactions of the Chinese Society of Agricultural Engineering*, 31(6), 35-41. http://dx.doi.org/10.3969/j.issn.1002-6819.2015.06.005